Sandia National Laboratories

Operated for the U.S. Department of Energy by
Sandia Corporation

Albuquerque, New Mexico 87185- 9111

date: October 10, 2002
Original February 21, 2000; revised May 4, 2000; revised October 10, 2002

to: Distribution

from: T.A. Baer, MS 0826, Org. 9111

subject: Computations for slot coater edge section (GT-013.3)

keywords: 3D, slot coater, free surface, static contact line, dynamic contact line, mesh, CUBIT, boundary conditions, rotated boundary conditions, solution procedure

input records: VELO_SLIP, VELO_NORMAL_EDGE, VELO_TANGENT_-EDGE, VAR_CA_EDGE, CAPILLARY, ROT SURFACE, ROT EDGE, ROT VERTEX

Introduction

An application of GOMA's three dimensional free surface modeling abilities is the edge portion of a slot coating device. Slot coating is a widely used operation for application of thin films to great lengths of substrate material, for example, photographic films. Because of the typically large difference in length scales between film thickness and substrate breadth, this operation is most often modeled in a simplified two-dimensional setting. Nonetheless, the influence of the coating flow in the vicinity of the slot coater edge can play an important part. This flow regime possesses complicated three dimensional fluid flow along with free surfaces and static and dynamic contact lines. GOMA is unique in its ability to contend with problems of this nature and this situation is a good demonstration of these capabilities.

There are several aspects to this memo. The creation and meshing of the initial solid model of the edge coater geometry will be described. This was accomplished using Sandia's meshing tool CUBIT. Details of the solid model creation will be included and the appropriate meshing sequence. Following this, we will delve into and describe the boundary conditions applied to the geometry. Aspects of the solution procedure are next. Followed by a sequence of computations which explore a little bit of the parameter space and the various behaviors observed.

Creating the Solid Model and Mesh

Figure 3 shows the solid model that was created to solve the slot coater edge problem. An exploded viewpoint with labels given to each of the subvolumes is also shown in Figure 3. Creation of the two "L" shaped volumes, began with a cylinder

of the appropriate length that was sectioned down the middle, leaving only a half cylinder. This was further reduced by using a cutting plane to shave off a small piece of the underside so a narrow flat region extended along the underside down the length of the cylinder. Another cutting plane slightly higher than the first but still parallel sectioned the doctored cylinder into a narrow longitudinal fillet. The end surfaces of these precursors were swept around in a 90 degree arc to create the elbows and further swept along a vector direction perpendicular to the original cylinder to create the perpendicular leg of the "L". Uniting all the volumes created in these sweep procedures left the two precursors volumes to volumes 1,2,6, and 7.

A brick of the appropriate dimensions that would fit inside the arms of the "L" was created next. The only subtly in its creation was that initially this brick overlapped the "L-shaped" volumes at the elbow. It was necessary to use the curved inner surfaces of this elbow as cutting tools to remove this overlapped region from the brick. The rounded corner is evident in Figure 3. Volume 4 was just a brick positioned appropriately.

Volumes 1, 2, 3, 5, 6, and 7 were created by sectioning the precursor volumes already created by a vertical z plane just downstream of the inlet port. All volumes were then imprinted and merged.

The meshing procedure was begun by meshing the end cap surfaces of volume 1 and volume 2. Meshing of volume 1's end cap surface had to be controlled carefully toensure the proper refinement near the contact line and especially that the contact line edge belongs to only one element at any point along its length. The latter requirement is a restriction imposed by GOMA's contact line algorithms. Meshing volume 1 and 2 applied CUBIT's sweep algorithm from one end cap surface to the to the other, that is, sweeping down one arm of the L and the out along the other. Enough elements in the elbow region were ensured by specifying a fixed (six) number of intervals along the inner elbow. curves.

Volume 4 was meshed by sweeping a mapped mesh from top to bottom. Volume 3 was then meshed by first creating a paved mesh on the portion of its upper surface that doesn't intersect volume 4 and then sweeping the whole volume from top to bottom. Volumes 6 and 7 were meshed by sweeping the surfaces where they intersect volumes 2 and 1, respectively, down their length, that is in the opposite direction in which volumes 1 and 2 were swept. The upper surface of volume 5 was mapped and then swept top to bottom to mesh volume 5. The final meshing of all volumes is shown in Figure 2.

Boundary Conditions Applied

Figure 2 shows a two point view of the geometry and indicates the nature and location of the boundary conditions applied. On the underside of the geometry, where the fluid phase adheres to the moving substrate, an essential condition is applied to the velocity so that no slip is enforced between the fluid phase and the substrate which is assumed

to be moving with velocity *(0, 0, -V_w)*. Surrounding this relatively large area, is a small, narrow region of elements adjacent to the contact line where the no slip condition between web and fluid is not so strongly enforced (sideset 100). Here a VELO_SLIP card is applied. The slipping parameter, β, was set to 0.01 to allow for moderate amounts of slip. The need for this region is two-fold. First, there is a need for a region were the velocity fields can "relax" from the values imposed by the wetting line physics (to be discussed shortly) and the no slip web speed region, and second, in order to impose these wetting line velocities, a region with a weak velocity condition is needed next to the contact line. Otherwise, the essential conditions would override the wetting line velocity conditions.

The conditions on the velocity field imposed by the wetting line have been discussed elsewhere[1]. Briefly put, it is assumed that the wetting line physics impose the requirement that the velocity of fluid at the contact line is everywhere tangent to the contact line. Thus, if n_{cl} is a unit vector normal to the contact line in the plane of the substrate and t_{cl} is a unit vector tangent to the contact line in the same plane, then the two conditions imposed are,

$$n_{cl} \cdot u = 0, \quad \text{and} \quad t_{cl} \cdot u = t_{cl} \cdot V_w \quad . \tag{EQ 1}$$

These two conditions are imposed using the VELO_NORMAL_EDGE and VELO_TANGENT_-EDGE boundary condition cards. An essential condition on the vertical velocity component is used to impose impenetrability on the contact line. The VAR_CA_EDGE condition was used to impose a contact angle on the contact line. The angle is determined from the relation

$$n_w \bullet n_{fs} = \cos\theta = \cos\theta_s - c_T Ca_L \tag{EQ 2}$$

where

$$Ca_L = -\frac{\mu(n_{cl} \bullet (V_w - \dot{x}_{fs}))}{\sigma} \tag{EQ 3}$$

However, in a number of the computations presented in this memo, we have chosen to ignore the influence of local velocity on contact angle and consequently set $c_T = 0$. The static angle, θ_s, was set to *168*, which was the initial contact angle occurring in the meshing solid model.

The boundary conditions applied to the liquid/air free surface are those typical to GOMA. The kinematic relation,

$$n \cdot v = 0 \tag{EQ 4}$$

is imposed on the mesh equations with the KINEMATIC card. Surface tension forces on this surface are introduced into the momentum equation via the CAPILLARY card.

It is important to the note that this card sets the external pressure on the free surface to a nominal, constant value (zero). This is true both up and downstream of the inlet feed slot. In some slot coating operations lowered pressures are applied to the upstream meniscus in an effort to stabilize the process at high processing speeds. In the geometry we have constructed, the upstream and downstream menisci are physically connected. Thus, the need for a constant external pressure.

The solid surfaces which make up the walls of the inlet feed slot and the horizontal "shoe" region are shown in Figure 3. The velocity of the fluid is set to zero on these regions. On the edge where the shoe contacts the kinematic free surface (the static contact line) the mesh nodes are constrained to fixed locations. In essence, this line is modeled as a sharp edge where the fluid has adhered.

The vertical boundary where the slot edge section would join the rest of the slot coater is modelled as a symmetry boundary. Components of velocity normal to it are prohibited by essential conditions; velocity components within the plane however are unconstrained. Similarly the mesh nodes are permitted to move within this plane but not normal to it by use of a PLANE command.

On the plane where the fluid exits the domain, essential conditions set the component parallel to the substrate plane equal to the web speed; zero shear conditions (natural conditions) are imposed on the other two fluid momentum components. Another PLANE command constrains the nodes at the exit to remain in their original plane. On the inlet plane, rather than attempt to impose an analytical solution to fully developed flow in a rectangular channel, a uniform inlet velocity is imposed across the inlet and the fully developed profile appears a little bit further on. Because the Reynolds number is small in all cases considered, this entry length is also short. The value for the imposed uniform velocity profile is chosen as a factor (often less than one) of the web speed.

It should be noted that whenever possible the PLANE commands alluded to above were actually PLANEX, PLANEY, or PLANEZ depending upon the orientation of the surface. Since the latter cards represent unrotated mesh constraints, it was unnecessary to include a ROT card for each of these planes. This simplified the Rotation Specifications section of the input deck.

An additional point that, while not related to boundary conditions, is an important aspect of the problem and needs to be brought out. There are in fact two element blocks used to solve the problem. The first block is a narrow "fillet" that encompasses a small region of the fluid adjacent to the contact line (volumes 1 and 7 in Figure 3). The second block is all the remaining domain. In both, the properties of the fluid are exactly the same, but the properties of the pseudo-solid material are not. In the fillet volume, we have set the shear modulus to be 10,000 times greater than the bulk modulus. In the rest of the volume, the ratio is one-tenth to one. The reason for this is that because of the mesh constraints imposed at the contact line, the region of the pseudo-solid adjacent to the contact line receives a great deal of localized "pseudo-stress." By choosing the

parameters in this region as we have, the elements can be made to resist shearing deformations more than elsewhere and hence preserve their integrity throughout the computation. Further, by confining this stiffer region to a small one near the contact line we avoid problems with poorly conditioned matrices that arise when there are significant differences between bulk and shear moduli.

A Word or Two about Rotation Conditions

Second only to domain construction and meshing, specification of the rotation conditions is the most difficult conceptual problem associated with 3D problems with GOMA. The necessity for rotation conditions arises from the fact that when applying penalized conditions (e.g. strong integrated conditions) to boundaries, spurious sources of tangential fluid or pseudo-solid momentum (forces) will appear at the surface if those forces are not restricted to directions which are normal to the local surface. Thus, it is the normal component of the appropriate momentum equation which must be replaced by the penalized constraint and it is the tangential components that must be retained to ensure that the forces tangential to the surface are null. Hence, the requirement for rotating the equations at surfaces where this class of boundary condition is applied.

It is the complexity of three-dimensional domains, however, that necessitates the specification of rotation conditions. In two-dimensions, things are sufficiently simple that an automated algorithm can be used to identify the appropriate BC that needs to appear at a given point on the boundary. In three dimensions, nothing is ever easy. Hence, it is left to the user to identify what boundary condition must be applied over those regions of the boundary where rotated boundary conditions are used.

An additional issue, is the ordering of boundary conditions appearing on a given ROT card. When using a direct solver, this ordering is immaterial, however, when using an iterative solver (which is most often the case in three dimensions) the order of boundary conditions can have a important impact on the structure of the matrix and ultimately the success or failure of the iterative solver.

Rotation conditions were discussed in considerable detail in [2,3] and here only a few salient rules in no particular order will be reiterated:

A ROT SURACE card is needed for all penalized rotated boundary conditions. Examples are KINEMATIC, VELO_NORMAL, PLANE, SPLINE. Weakly applied boundary conditions like VELO_SLIP or CAPILLARY do not need ROT cards.

For the greatest robustness, ROT SURFACE, EDGE, and VERTEX cards should be included for all such entities where rotated boundary conditions are applied.

In general, all SURFACE ROT cards will include a single boundary condition and two tangent vector entries. EDGE ROT cards will typically include the two boundary conditions contributed by the sidesets forming the edge and a single tangent vector entry. VERTEX ROT cards typically include only the three boundary conditions associated with the three sidesets that form the vertex.

The rotated boundary conditions that are applied at a given point are determined by the following precedence rule: First VERTEX ROT card in the file that applies to that point, then first EDGE ROT card, then first SURFACE ROT card.

Dirichlet conditions applied at a point override all boundary conditions specified by ROT cards for that point.

For rotated conditions applied to surfaces the user must help GOMA define a rotated basis by specify a seed vector or a method of choosing a seed vector. When selecting a SEED vector for a surface ensure that it is never normal to any point on the surface. For curved surfaces, it is better to use the BASIS_RESEED method for choosing the tangent vectors. SEED vectors are very rarely needed for ROT EDGE and ROT VERTEX cards.

For rotated conditions applied at edges, the rotation basis is determined by finding the direction vector along the edge (this is the T 0 direction), the outward normal of the primary (first) sideset appearing on the ROT card and the cross product of these two vectors (the B 0 direction). Thus, the rotated basis appears naturally from the geometry and use of SEED vector for EDGE cards is rare.

The ordering of boundary conditions with a given ROT card should be such that the constraints are associated with the spatial direction to which they are most sensitive. Thus, the first boundary condition should be most sensitive to the x component of the appropriate degree of freedom (be it velocity or mesh displacement), the second boundary condition most sensitive to the y component, and the third condition most sensitive to the z component. This is the reason that PLANE conditions associated with planes of constant x should be placed in the first spot, PLANE conditions associated with constant y should be placed second, etc. Of course, this rule cannot always be strictly applied. For example, curved free surface boundaries can be sensitive to all three directions at once.

Boundary conditions that are applied to edges, e.g. VELO_NORMAL_EDGE, CA_EDGE, VAR_CA_EDGE, typically will need to included in a ROT EDGE card since it is almost always the case that some surface boundary with a rotated boundary condition will include that edge. Failure to include this card will result in the EDGE conditions not being applied.

PLANEX, PLANEY, and PLANEZ are unrotated PLANE constraints that identify a given sideset as being a plane of constant x, z, or z, respectively. These cards do not need rotation specifications and hence should be used liberally when assigning boundary conditions since they provide considerable simplification of the Rotations Specifications section.

Dimensionless Groups

For greater generality (at the expense of increased obscurity) the equation set solved was first cast in terms of dimensionless variables, based upon the web speed as a velocity scale and the slot width as the dimension scale. This naturally leads to a set of

dimensionless groups which define and related the physics that are appropriate to each problem. The first is the Reynolds number,

$$Re = \frac{\rho V_w L}{\mu} \quad \text{(EQ 5)}$$

where V_w is the speed of the web and L is the width of the slot feed. The second, the capillary number, is essentially a dimensionless surface tension:

$$Ca = \frac{\mu V_w}{\sigma} \quad \text{(EQ 6)}$$

where σ is the surface tension. Gravitational influences appear in the Stokes number,

$$St = \frac{\mu V_w}{\rho g L^2} \quad \text{(EQ 7)}$$

The Bond number is the ratio of capillary to Stokes number and expresses the relative sizes of gravitational and surface tension forces,

$$Bd = \frac{Ca}{St} = \frac{\rho g L^2}{\Gamma} \quad \text{(EQ 8)}$$

This number will turn out to be associated with certain behaviors observed in these computations.

Finally, dynamical behavior of the system is to a certain extent fixed by the ratio of the inlet average velocity to the web speed, which we have given the label α:

$$\alpha = \frac{\langle V_{in} \rangle}{V_w} \quad \text{(EQ 9)}$$

Aspects of the Solution Procedure

As is usually the case, the initial step in obtaining a solution to this problem is to compute a velocity/pressure solution on the fixed mesh depicted in Figure 2. In this step, the surfaces which are ultimately free surfaces have VELO_NORMAL boundary conditions imposed. This card imposes the identical constraint as the KINEMATIC card with the exception that it replaces the normal component of the momentum equation, rather than the mesh equation. Since the mesh unknowns are not included in this initial computation, the mesh is fixed. Consequently, the VELO_NORMAL card will impose appropriate pressures on the boundary to ensure that the velocity vectors are consistently tangent to it throughout. At the contact line, the

VELO_NORMAL_EDGE and VELO_TANGENT-_EDGE cards are also applied. An additional point is the necessity of consistency between the imposed inlet and outlet velocities. Since the mesh cannot alter its shape at the exit plane to account for any discrepancy, it is important at this stage to impose an inlet velocity such that the inlet to outlet velocity ratio is consistent with the inlet to outlet area ratio. Consequently in this computation, α is not a free parameter but instead must be the ratio of the outlet to inlet area. Note that this requires a separate computation for inlet and outlet areas.

With a successful computation of the fixed mesh velocity and pressure fields, a solution for the moving mesh can be begun with it as a starting point. However, since GOMA makes use of a full Newton-Raphson scheme, care must be exercised at this point. The mesh nodes initially are far away from their final positions, consequently the "pseudo" forces on the "pseudo-solid" are quite large and apt to produce huge displacements during the initial iterations. Since no constraints exist on the smoothness of the mesh surface, the net effect is gross distortions in the mesh commonly referred to as the "rat in the microwave" result. To counter this, the damping factor is set to a very small value, often as small as 0.05, so that the mesh nodes will displace only a very small fraction of that indicated by the "pseudo" forces. In this fashion, often after 50 to 100 iterations, the initial mesh is gradually distorted until it reaches the "vicinity" of the final converged answer. At that point, the mesh nodes are near enough to their final locations, that the damping parameter can be returned to unity and full, undamped Newton iterations can be applied to bring the solution to its final convergent state in only a few iterations.

Once a convergent solution is obtained, additional solutions in the parameter space may be obtained via continuation.

Computational Results

Influence of the Inlet Speed

The first parameter to be considered was the effect of changing the inlet average flowrate while keeping the web speed constant. The capillary number was fixed at *2.0*, the Stokes number at *1.02*, and the Reynolds number at *0.01.* The starting point for this computation was the solution that had been relaxed with $\alpha = 1.59$ from the fixed mesh solution, which was computed with the same value for α.

From $\alpha = 1.59$ the solution was continued downward in α until a value of *0.815* was reached. At this point, the mesh had become too distorted to continue. Figure 3 shows the shape of the free surface around the slot edge at four values in this range. Generally, as the inlet flowrate is decreased the free surface contracts inward with the upstream portion of the contact line moving downstream nearer the plane of the slot. Downstream, the contact line actually contracts inward forming a question mark shape. Because this contraction is accompanied by a slight hump in the free surface as it leaves the domain, we speculate that this behavior is the result of surface tension forces. At very high *Ca*, the contact line might not contract inwards at all.

It should be noted that at the lower values of α the mesh in the vicinity of the static contact line has become quite distorted. This is a consequence of pinning the mesh nodes to the original curve. A more realistic computation would be to allow this set of mesh nodes to move along with everything else, but maintaining a constant contact angle. This separate computation will be discussed later.

Influence of Reynolds number

The effect of the fluid inertia on the free surface shape was considered by, of course, varying the Reynolds number. However, in the initial set of computations we did not vary the Reynolds number directly but instead varied the web speed while keeping the capillary number fixed at *2.0*. The Stokes number was computed from the web speed via (7) with the net effect being to change the relative proportion of gravitational forces to surface tension, *i.e.* the Bond number. This had unforeseen but ultimately illustrative consequences.

Figure 4 shows results at four values for *Re*: *0.01, 0.05, 0.1,* and *0.5*. The most interesting feature is the thickening of the free surface near the contact line as it leaves the downstream end of the domain. For the lowest value of *Re*, the upper portion of the free surface leaves the domain as a nearly flat sheet. However, as *Re* increases the upper portion takes on decidedly more contour and at the same time the contact line moves inward towards the symmetry plane. Originally this behavior was thought to relate to the increasing Reynolds number, however, we have included in Figure 4 values for *St* which vary from *1.02* to *50.0* as *Re* increases. Since the capillary number is a constant, this implies that the Bond number is decreasing. That is, gravitational forces are declining with respect to capillary forces with the observed effect that the free surface is being pulled inwards towards the symmetry plane as the influence of surface tension increases.

That this "heavy bead" behavior is a function of the Bond number is reinforced by a second set of computations illustrated in Figure 5. Here both *Ca*, *St* and α are fixed at *2.0, 0.98,* and *1.59*, respectively, and *Re* is varied independently. The figure shows results for *Re = 0.015, 0.10, 0.25* and *0.35*. Although, there are slight differences in the free surface shape they are not discernible in this figure. The clear indication being that Re has little effect over this range in its value.

Influence of Increased Processing Speed

A final sequence of calculations explored the effect of increasing the processing speed on the shape of the slot coater edge free surface. In this calculation, we abandoned expressing the results solely in terms of dimensionless groups and instead consider the behavior of a fluid with the following (dimensional) properties: density, *1* g/cm^3; viscosity, *1000* cP; surface tension, *50* dyn/cm. The speed of the web was varied from *10* cm/s to *50* cm/s with the inlet flow rate also increased so that α would be fixed at *1.59*. The width of the inlet channel was *1* mm.

Figure 6 shows the results at web speeds of *10, 20, 40* and *50* cm/s. The most interesting thing observed is that the "heavy bead" begins at a location relatively near the symmetry plane. It also extends vertically to height that is quite a bit larger than the distance between the slot coater shoe and the substrate, that is, the gap. However, as the processing speed increases the height of this feature diminishes and its location moves outward. In the figure, we have included values for Re, Ca and St at each web speed. Since all three vary directly with web speed, they all likewise increase.
However, the Bond number is independent of web speed and remains fixed at *5.0*. However, the relative size of fluid inertia and surface tension, given by *ReCa*, clearly increases by a large degree as processing speed increases.

Interestingly enough the shape of the free surface upstream and lateral to the slot coater shoe is relatively unaffected by the increase in web speed. Including this observation with results shown in Figure 3 suggests that its shape is predominantly a function of the relative size of the inlet flow rate and web speed.

Unpinning the static contact line

This section describes an extension of the slot coater edge problem discussed above. Formerly, the static contact line, that is, the curve where the fluid adheres to the non-moving portions of the solid boundaries, was fixed in space. It therefore represented in some sense a discontinuity of the die geometry where the fluid adheres to but cannot wet past. A different situation arises if the static contact line is allowed to move being constrained only to stay in a specific plane and to adhere to that the plane at a specific, fixed contact angle at all points. This is referred to as an unpinned static contact line and perhaps is a more realistic representation of slot coating flows.

For the most part, this problem was approached in the same manner as described in the preceding sections. However, because two contact lines are now present a new decomposition to the geometry and new meshing was warranted to provide new element blocks in the vicinity of the static contact line which would allow for targeted mesh refinement and different pseudo-solid material properties for the reasons cited above. Figure 7 depicts the new meshing decomposition. It resembles that shown in Figure 3 except for the addition of an new, upper fillet volume adjacent to the static contact line. As before, a stiffer pseudo-solid material will occupy this fillet volume to mitigate distortion around the static contact line.

The no displacement boundary conditions formerly associated with the static contact line are replaced by a DY constraint and a CA_EDGE constraint that fixes the angle between free surface and the upper, solid boundary. In the computations to be shown, this angle was set at approximately *168* degrees.

Figure 8 is the counterpart to Figure 3 in that it depicts the response of free surface shape to average inlet velocity for the unpinned static contact line case. Both top and underside views are shown for three different flow rates: α = *1.96, 1.51*, and *1.22*. Because the static contact line is free to move outward, in this set of calculations it was possible

to increase α beyond is nominal value of *1.59*. Conversely, as soon as the contact line came into proximity of the inlet channel the computation could not continue. Consequently, $\alpha = 1.22$ was the minimum inlet to web speed ratio obtained. One can clearly see how close the static line is to the inlet in Figure 8.

Figure 9 shows the response to processing speed. The fluid's material parameters were described previously and the ratio of inlet to web speed was fixed at *1.59*. The figure shows the response at several web speeds ranging from *10* cm/s to *70* cm/s with an unpinned static contact line. By and large, the free surface shape upstream of the lower meniscus shows little response to the faster moving web, since the inlet rate is increased simultaneously. However, the downstream portion of the flow shows the identical trend observed previously when the static contact line was pinned: the heavy bead feature diminishes in height and moves outward.

Figure 10 and Figure 11 show the effects of changing *Ca*. In the first figure the static contact angle was fixed at a "non-wetting" value of 168° with a value of $c_T = 0.0$. Thus, the contact is fixed at 168° at all points on the dynamic contact line. It should also be noted that this same angle is also applied at all points on the static contact line. The Reynolds number and Stokes number were both fixed at *0.01* and *1.0*, respectively. The inlet to web speed ratio was also fixed at *1.59*. What is observed as *Ca* is decreased is that the downstream portion of the free surface tends to retract inward and increase in height. This we tend to explain as surface tension forces becoming dominant with respect to gravitational forces, i.e. *Bn* decreases.

When the static contact angle, however, is set at the "wetting" value of 45° for those cases shown in Figure 11, the trend with *Ca* reverses. That is, the free surface tends to move outward and become flatter as *Ca* and *Bn* decrease. It should be noted that in this latter sequence of calculations a non-zero value of $c_T = 0.842$ was used in a break with convention. This was done in part to mitigate mesh distortion at the leading edge of the flow domain. The reader can now see how the leading edge contact angle is decreasing with decreasing *Ca*, consistent with (2). Nonetheless, the trend was observed to be the same even with $c_T = 0.0$: the dynamic contact line moves outwards with decreasing *Ca*. Note the same static value for contact angle, 45°, was applied on the static contact line.

Conclusion

This memo has outlined the use of GOMA in approaching the simulation of a flow geometry representative of conditions near the edge of a slot coater. Solid model construction, domain meshing, and boundary condition placement were dealt with appropriately. A relatively brief study was undertaken to explore the response of the system to various changes in operating parameters and/or fluid properties. It was by no means exhaustive. Following this text, is an appendix which contains examples of the input files used to perform this analysis. It should assist the user who is interested in performing similar analyses.

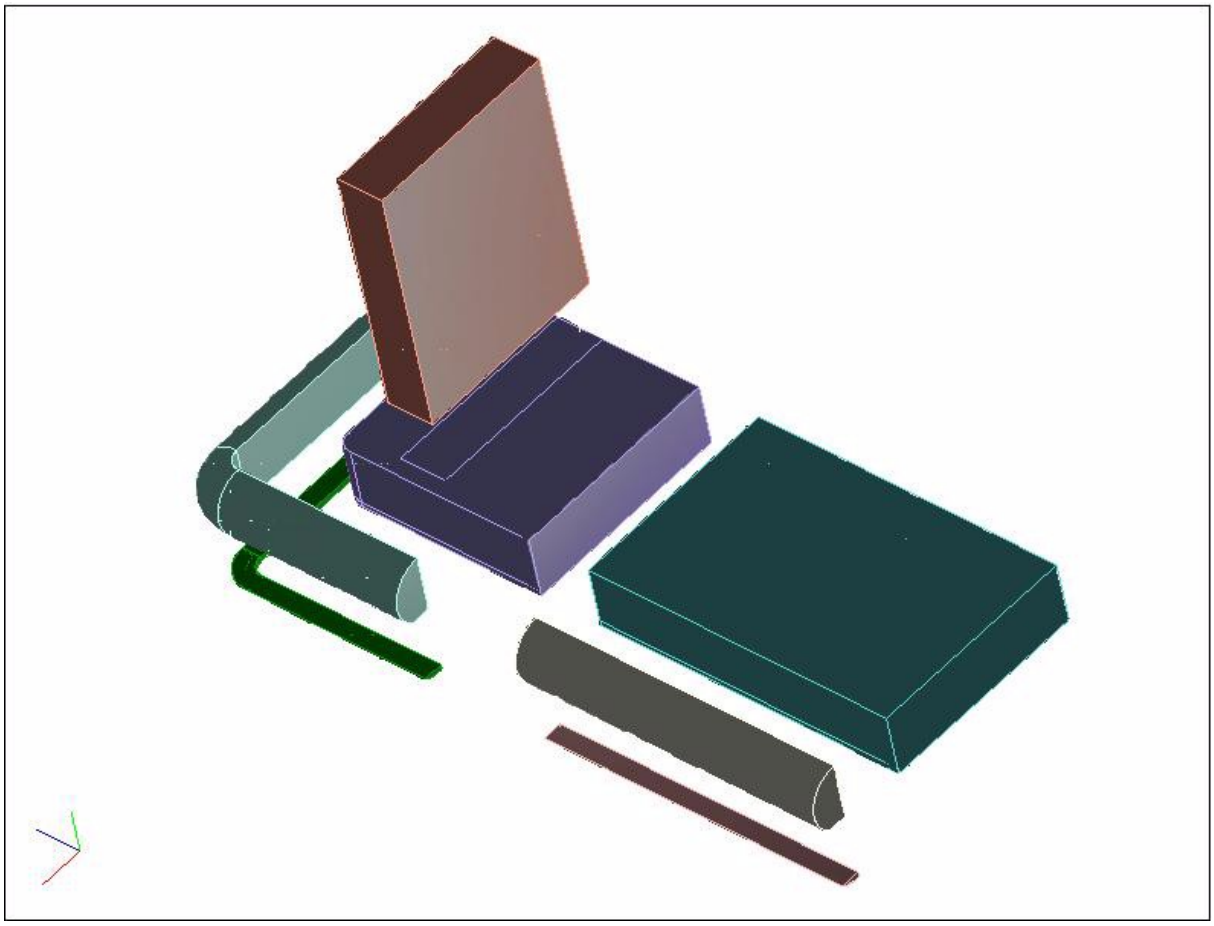

Figure 1. Exploded view of meshing decomposition of slot coater edge section geometry.

References

1. Baer, T.A., R.A. Cairncross, P.R. Schunk, R.R. Rao, P.A. Sackinger, "A Finite Element Method for Free-Surface Flows of Incompressible Fluids in Three Dimensions, Part II: Dynamic Wetting Lines," Int. J. Numer. Meth. Fluids, to appear 2000.

2. Baer, T.A.," Tutorial on droplet on incline problem (GT-007.2)," Internal Sandia memo,Sandia National Laboratories, July 30, 1999.

3. Schunk P.R., and P.A. Sackinger, R.R. Rao, K.S. Chen, R.A. Cairncross, T.A. Baer, D.A. Labreche, "GOMA 2.0, - A Full-Newton Finite Element Program for Free and Moving Boundary Problems with Coupled Fluid/Solid Momentum, Energy, Mass and Chemical Species Transport: User's Guide," SAND97-2404, Sandia National Laboratories, Albuquerque, NM, (1997).

Figure 2. Meshing and boundary condition description for slot coater edge section.

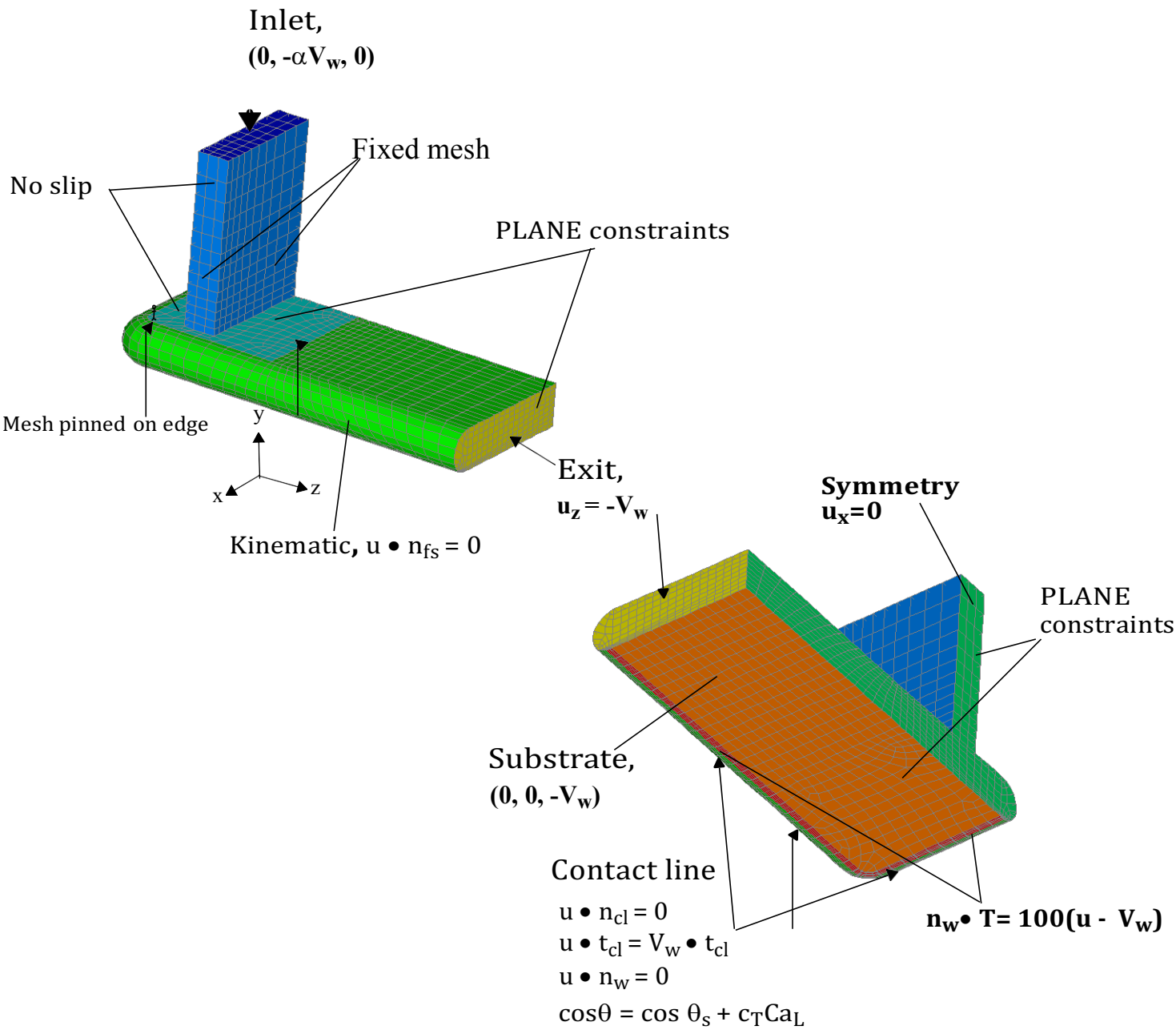
Inlet,
(0, -αV_w, 0)
Fixed mesh
No slip
PLANE constraints
Mesh pinned on edge
y
x
z
Exit,
u_z = -V_w
Kinematic, u • n_fs = 0
Symmetry
u_x=0
PLANE
constraints
Substrate,
(0, 0, -V_w)
Contact line
u • n_cl = 0
u • t_cl = V_w • t_cl
u • n_w = 0
cosθ = cos θ_s + c_T Ca_L
n_w• T= 100(u - V_w)

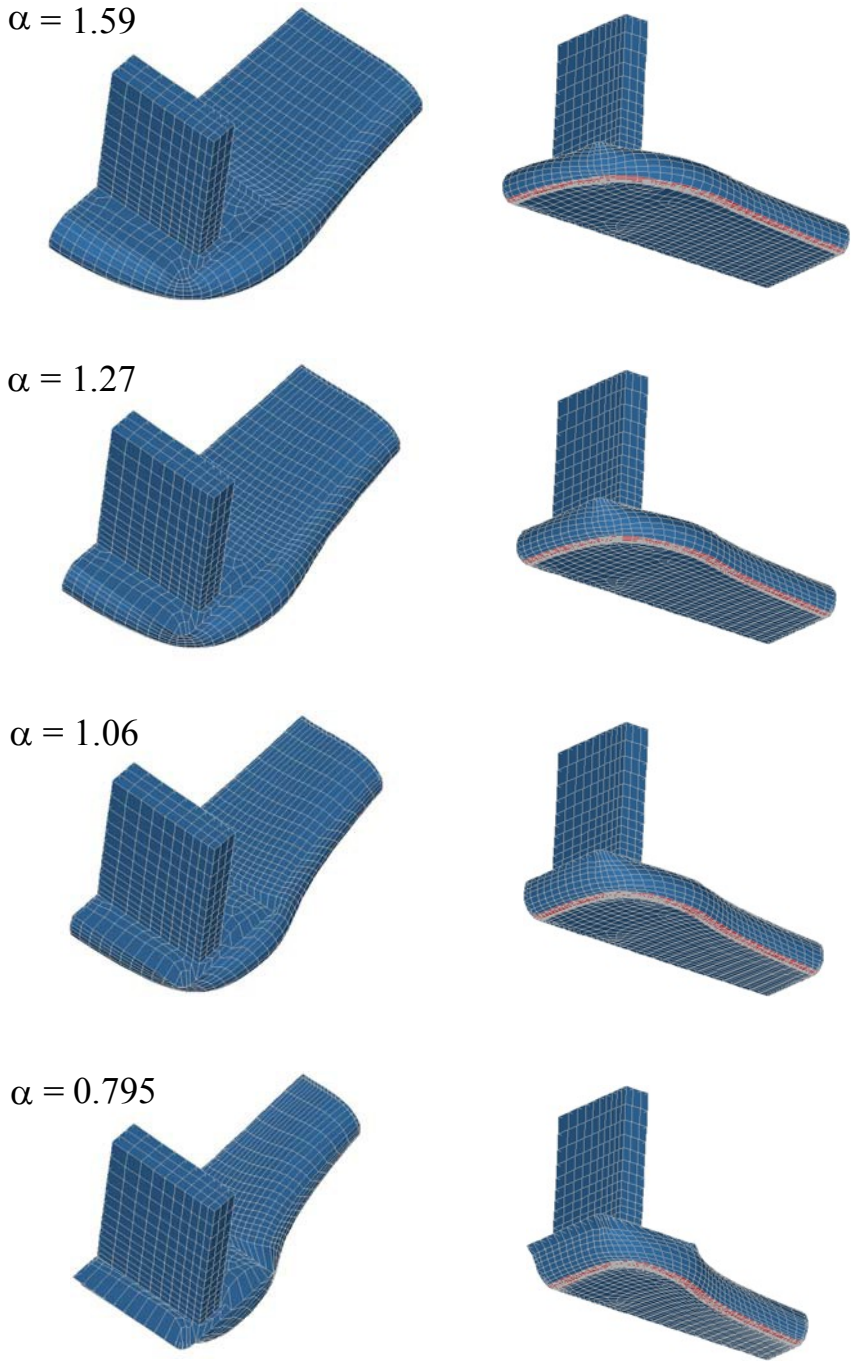

Figure 3. Influence of inlet average velocity to substrate speed ratio, α. *Re=0.01, Ca=2.0, St=0.98*. Note distortion of mesh in the vicinity of the fixed static contact line.

Re=0.01
St = 1.02
Bn = 2.0

Figure 4. Inadvertent illustration of the effects of increasing Bn number. *Ca=2.0,* Note the heavy bead feature increases in height and moves inward as Bn increases.

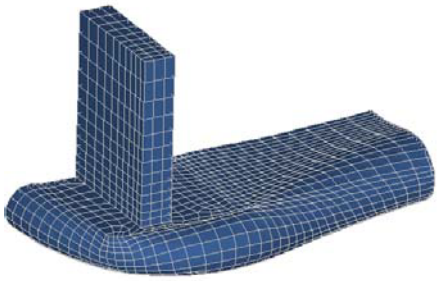

Re=0.05
St = 5.10
Bn = 0.392

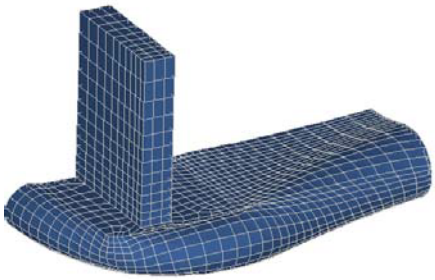

Re=0.1
St = 10.20
Bn = 0.196

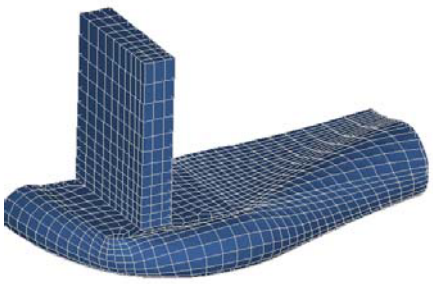

Re=0.5
St = 50.0
Bn = 0.04

Figure 5. Effects of increasing Re at constant *St=0.98* and *Ca = 2.0*. Note that *Bn = 2.04*. There are slight differences in these depictions, however, they are not visually apparent.

Re=0.015

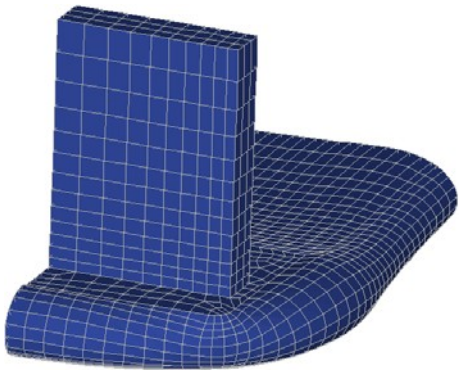

Re=0.10

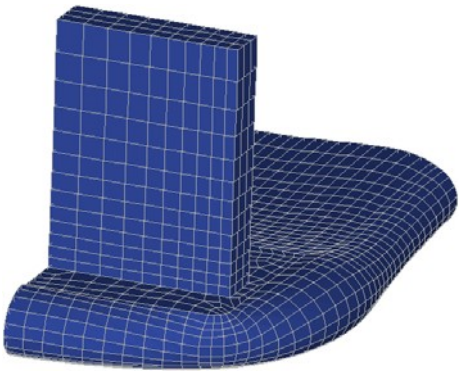

Re=0.25

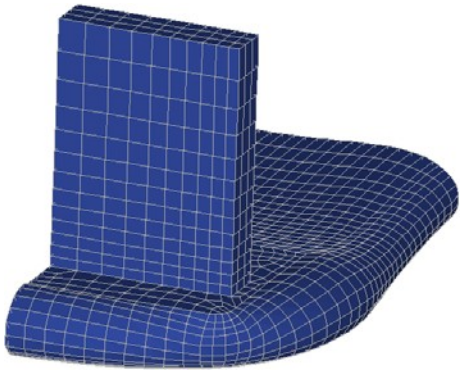

Re=0.35

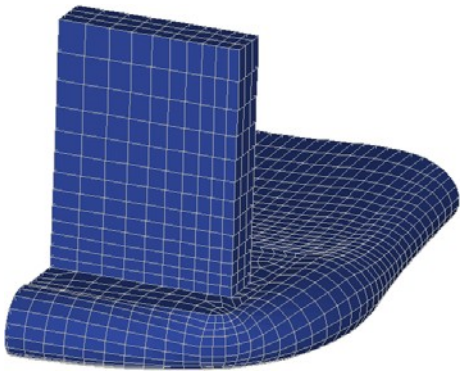

Figure 6. Effect of increasing process- ing speed. Ratio of inlet average velocity to web speed is fixed at *1.59* and web speed is increased as shown.

Re = 0.10
Ca = 2.0
St = 10.2

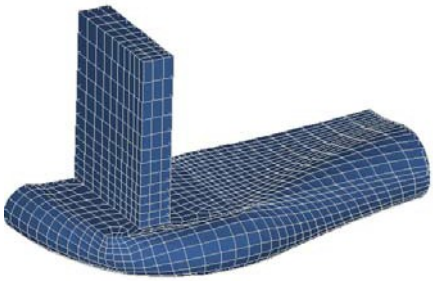

V_w=10 cm/s

Re = 0.20
Ca = 4.0
St = 20.4

V_w=20 cm/s

Re = 0.40
Ca = 8.0
St = 40.8

V_w=40 cm/s

Re = 0.50
Ca = 10.0
St = 51

V_w=50 cm/s

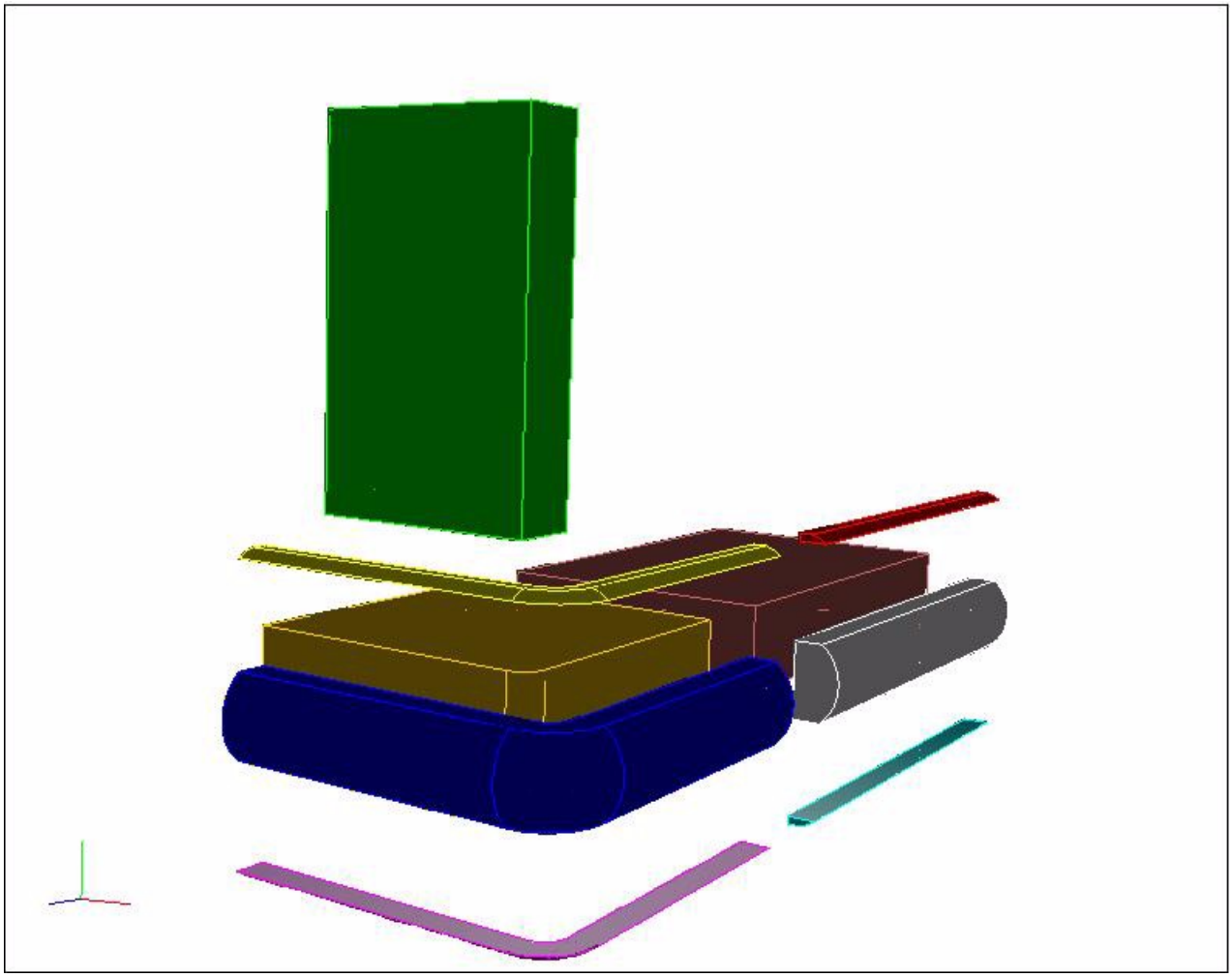

Figure 7. Meshing domain decomposition to permit unpinned upper static contact line.

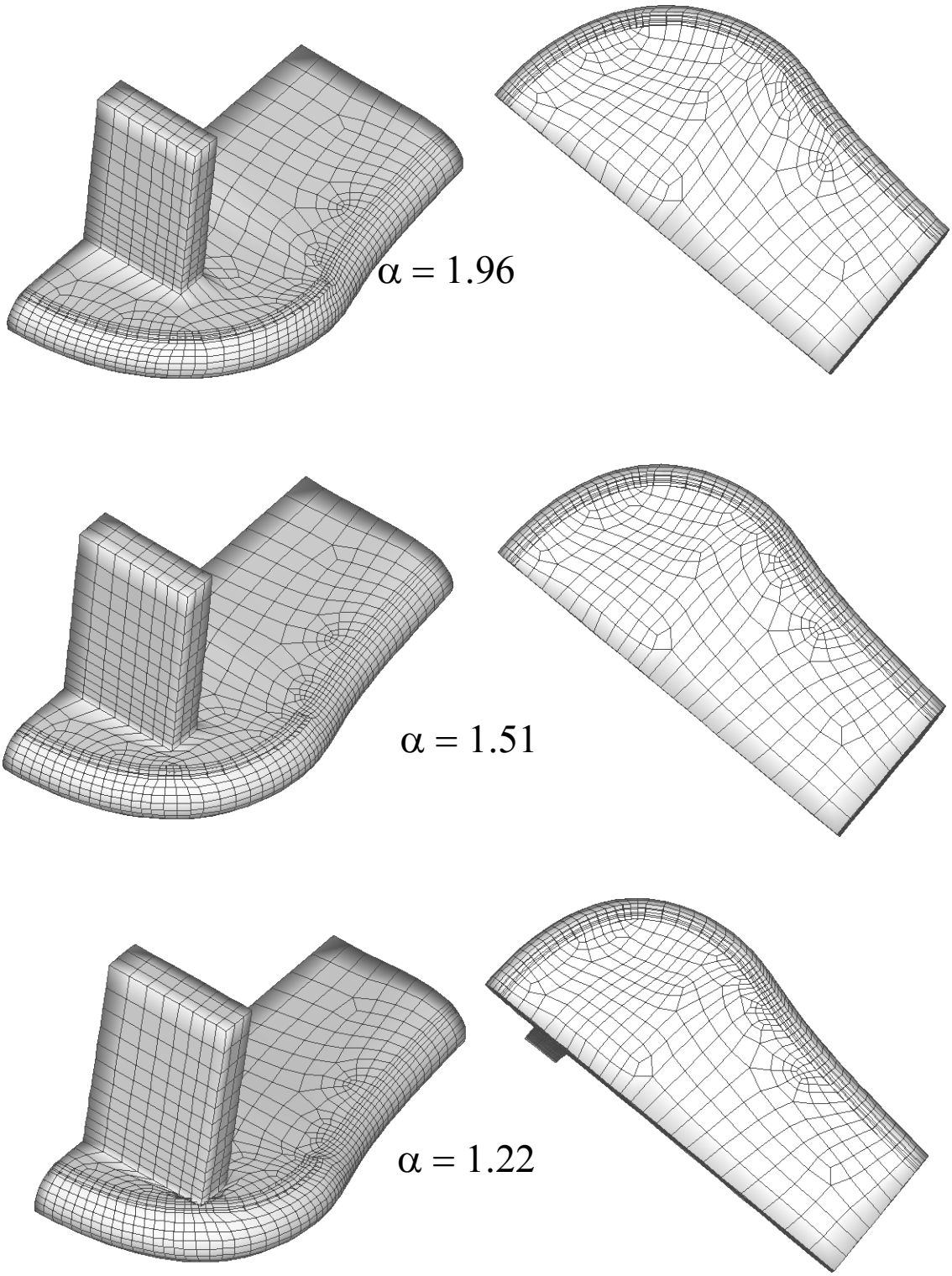

Figure 8. Effect of inlet average velocity to web speed ratio on free surface shape when upper contact line is unpinned

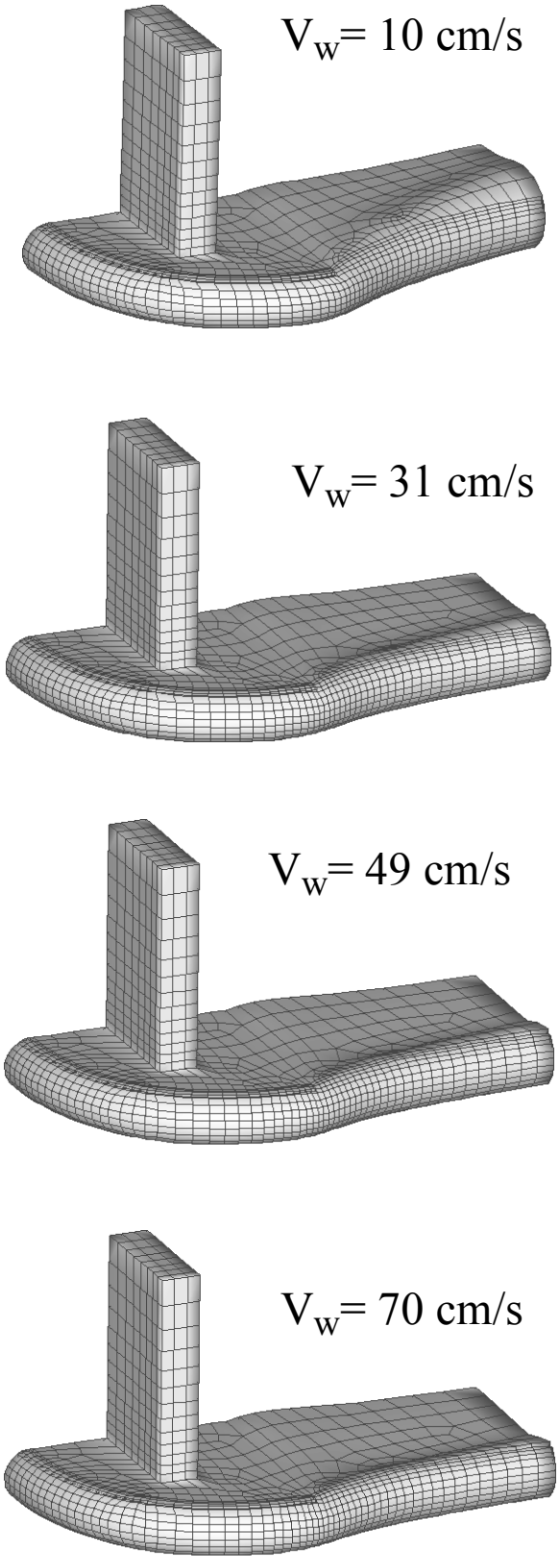

Figure 9. Influence of increased web speed. Note that the average inlet flow rate is increased to maintain a constant ratio with web speed. This ratio is fixed at *1.59*. The fluid flow parameters were given in the text.

Figure 10. Influence of Ca on free surface shape for non-wetting (> 90 ˚) static contact angle. *Re=0.01*, *St = 1.0*, α = *1.59*. Static contact angle is *168* ˚

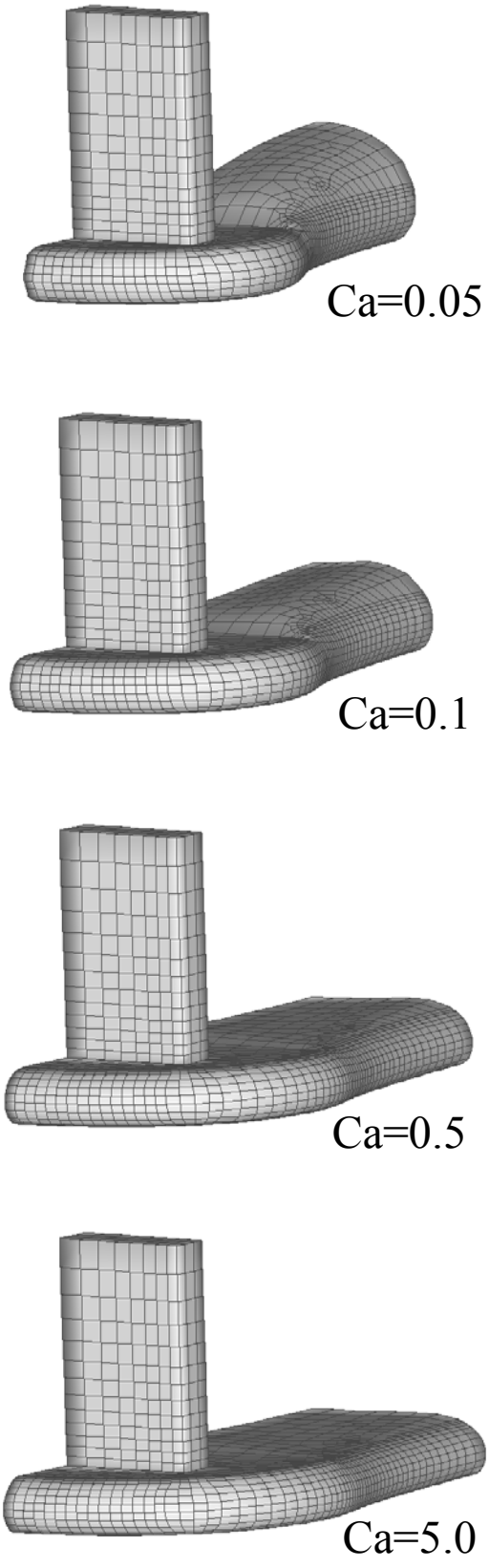

Figure 11. Influence of Ca on free surface shape for wetting (< 90°) static contact angle. *Re=0.01*, *St = 1.0*, α = *1.59*. Static contact angle is *45*°. Note that the range of Ca is smaller than in the previous figure since the degree of mesh distortion for this set of parameters is by and large greater.

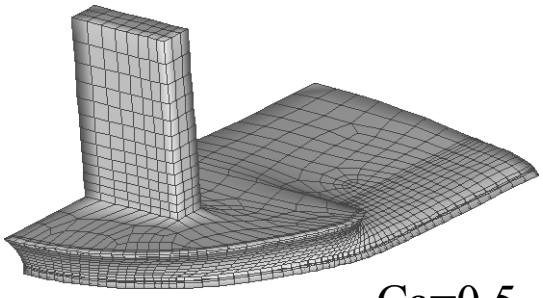

Ca=0.5

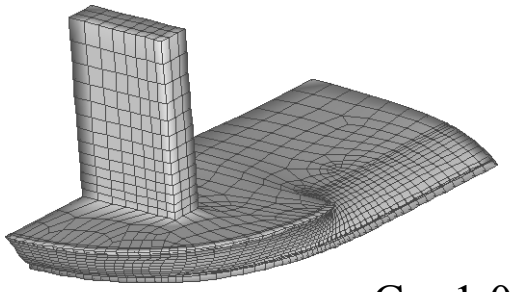

Ca=1.0

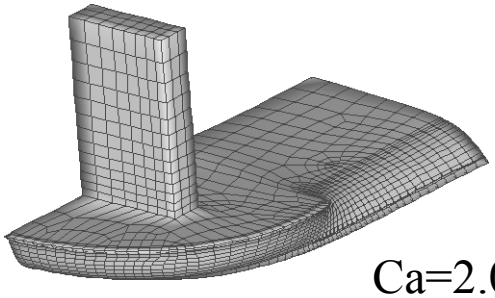

Ca=2.0

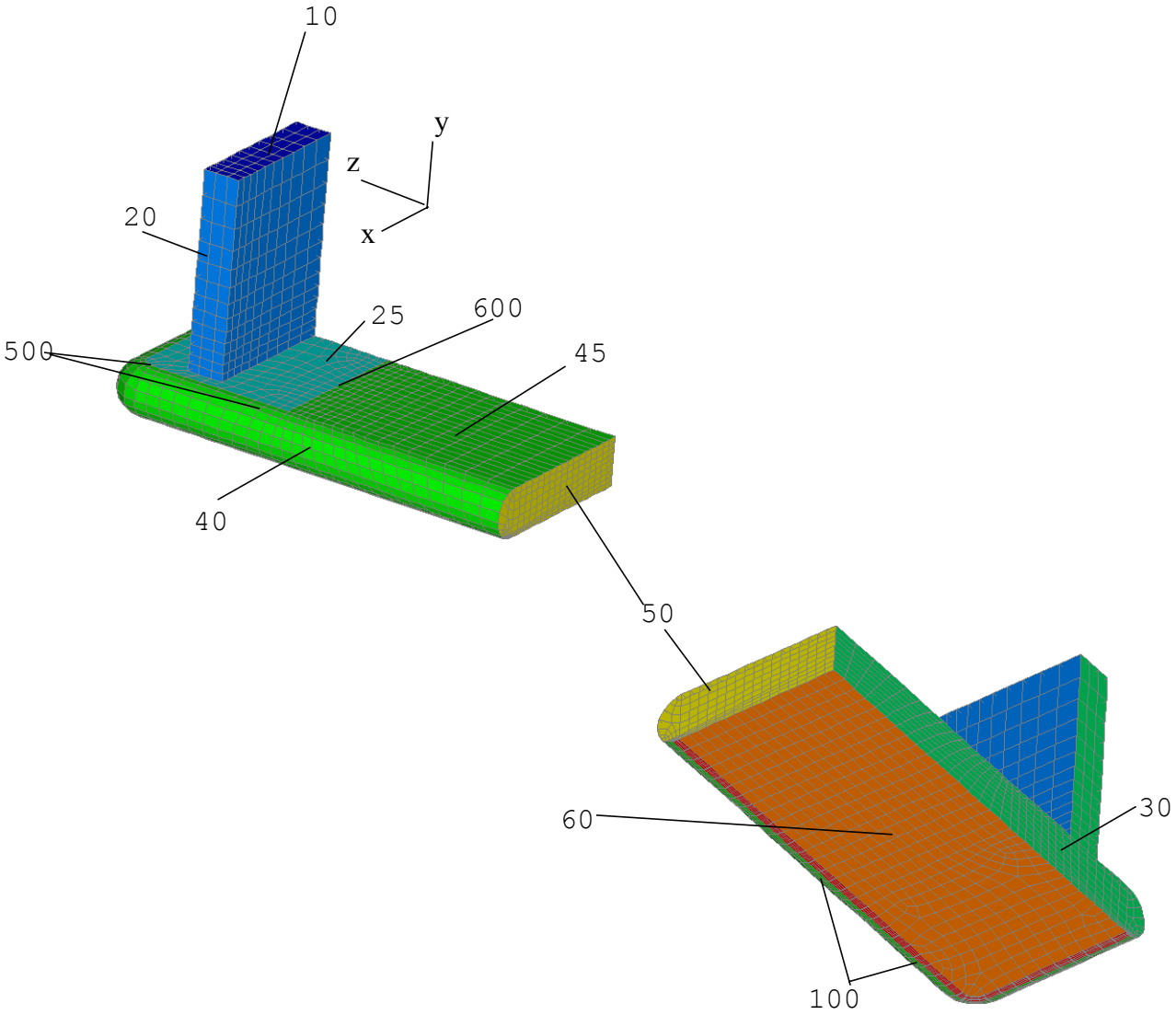

Figure 12. Side set and nodeset set designations for slot coater edge section. Note the sidesets and nodesets share the same designation, i.e. sideset 10 and nodeset 10 refer to the same geometrical entity. The exception is sideset 60 which compasses both the elements belonging to nodeset 60 and also sideset 100.

APPENDIX

In this appendix appears a sequence of input files to CUBIT and GOMA which were used to solve the unpinned static contact line problem. First, there are two CUBIT input files which create the solid model of the geometry and then mesh it appropriately, respectively. Following this is a file where the Aprepro definitions are kept. This is were the physical parameters to the problem are set and where the appropriate dimensionless groups are determined. After this is the actual GOMA input deck with is information regarding solver specifications, boundary conditions and the all important rotation conditions. Figure 12 should be used help interpret this input deck in regards to where each boundary condition or rotation condition is applied. Finally, an example material file appears is given.

Boundary Conditions and Rotation Specifications

This will be a brief discussion of some of the salient points concerning the list of boundary conditions and rotation specifications in the input deck included in this appendix. Having solved a number of problems with GOMA, the reader will be familiar with most of the BC cards listed. One of the unique features of this input deck are the conditions to contend with the static and dynamic contact lines. The fluid velocity at the dynamic contact line are set using VELO_NORMAL_EDGE and VELO_TANGENT_EDGE along with an essential condition on the velocity component normal to the web surface. We also note the VELO_SLIP card associated with sideset 100. This sideset is a narrow strip of elements adjacent to the dynamic contact line, seen in Figure 12. The reasons for this region were discussed above. Of course, there are no special velocity conditions associated with the static contact line. After all it is a "static" contact line and the fluid is assumed to not slip at all points along it.

The conditions to impose the boundary conditions on the mesh are also unique to this problem. In general the consist of a PLANEY card or DY card to fix the contact line points in the appropriate plane and either a VAR_CA_EDGE card or a CA_EDGE_INT card to specify a dynamic or static contact angle around the respective contact line. Note the six float values that appear at the end of the VAR_CA_EDGE card. These are the components of the substrate velocity and the normal vector to the substrate, respectively. An additional point is that we use nodeset 500 which is a line of nodes that coincide with static contact line around the shoe of the slot coater(see Figure 12) to constrain the y motion of the static contact line. Nodeset 600 is a subset of nodeset 500 and consists of the nodes on the line the downstream transverse portion of the static contact line. The mesh nodes are fixed by DY and DZ essential conditions on this nodeset.

For such a complicated problem, the Rotation Specifications section is relatively short. There is a ROT MOM condition for the dynamic contact line edge where the VELO_NORMAL_EDGE, VELO_TANGENT_EDGE and essential V velocity cards are identified. This card is included primarily to ensure that these boundary conditions are unequivocally applied on the dynamic contact line. There is only one other surface that

possesses a rotate mesh constraint and that is the free surface and KINEMATIC constraint. Hence, we need only a single MESH SURFACE ROT card. Note that choice of seed vector selection is set to BASIS_RESEED which experience has indicated as the most robust method for surfaces that curve in all three dimensions. The placement of the KINEMATIC card at the central, y, position was for the most part arbitrary since the KINEMATIC constraint is sensitive to all three displacements to varying degrees over its entirety. In situations like this, trial and error is often the most effective approach.

The EDGE ROT cards are used to guarantee the set of boundary conditions applied along a "seam" between adjacent side sets having different (or identical) boundary conditions. If one considers the slot coater edge geometry, there are four such seams where the free surface and its KINEMATIC constraint intercept other geometric elements. 1) dynamic contact line, 2) the static contact line, 3) the intersection with the symmetry boundary (SS 30), 4) the intersection with outlet plane (SS 50). An interesting point to bring out is the boundary conditions applied on the static contact line. The EDGE card for this edge indicates the following three boundary conditions:

T 0 DY 500 CA_EDGE_INT 40

However, as noted above, nodeset 600 applies essential conditions on DY and DZ. Consequently, for nodes on this nodeset the boundary conditions applied would be actually:

T 0 DY 600 DZ 600

Thus, for nodes on nodeset 600 no contact angle constraint is applied. Instead, the nodes can move only in the x direction and since the tangent direction of this edge also coincides with the x direction, this also implies zero force applied on this edge in the x direction.

The last section of the Rotation Specifications area lists several ROT VERTEX cards. As the name implies these cards specify the boundary conditions applied at a vertex point where several sidesets intersection. Since several EDGE and SURFACE ROT cards could conceivably apply to such a point it is important to make unambiguous exactly the BC's that should be applied there. In the case of the slot coater edge there are five such vertices: 1) one where the dynamic contact line intersects the symmetry plane, 2) another where the dynamic contact line intersects the exit plane, 3) two points were the static contact line intersects the symmetry plane, 4) and the intersection of the kinematic surface, the exit plane, and the symmetry plane. Notice that a vertex card exists for all five vertices. In practice, VERTEX cards are sometimes redundant; the previous SURFACE or EDGE cards are often enough to provide appropriate boundary conditions specification. However, this is not always the case. When a problem is not working correctly, for example, when the initial few iterations produce those well-known unphysical mesh distortions, it is well worth it to view the distortion with a very small magnification factor in BLOT. It is often the case that the origin of the distortion is at a vertex which needs a VERTEX ROT card.

CUBIT - solid model construction file:

```
cylinder radius 0.5 z 8
webcut body 1 with plane xplane
delete body 3
create surface from surface 5
sweep surface 12 axis -0.25 0 4 0 1 0 angle -90
sweep surface 15 vector -1 0 0 distance 3
unite body 2 with body 6
webcut body all with plane yplane offset -0.48
delete body 8
webcut body all with plane yplane offset 0.48
delete body 11
webcut body all with plane yplane offset 0.4
webcut body all with plane yplane offset -0.4
brick 3.25 0.96 8.25
brick x 3.25 y 0.96 z 8.25
body 16 move -1.625 0 0.125
create surface from surface 102
create surface from surface 93
create surface from surface 84
unite body 17 18 19
webcut body 16 with sheet surface 117
delete body 22 20
brick x 2.5 y 4 z 0.75
body 23 move -2 2.48 3
webcut body all with plane zplane offset 1
body all move 3.25 0.48 -3
export acis "edge_coat5.sat"
```

CUBIT - meshing file:

```
import acis "edge_coat5.sat"
imprint all
merge all
surface 22 36 size 0.04
surface 22 36 scheme pave
surface 52 size 0.15
surface 52 scheme pave
mesh surface 22 36
mesh surface 52
curve 47 scheme bias 1.05 start vertex 11
curve 44 scheme bias 1.05 start vertex 9
curve 41 scheme bias 1.05 start vertex 10
curve 43 scheme bias 1.05 start vertex 12
volume 3 size 0.25
volume 3 scheme sweep
volume 3 scheme sweep source surface 22 target surface 7
mesh volume 3
curve 80 scheme bias 1.05 start vertex 33
curve 77 scheme bias 1.05 start vertex 34
volume 7 size 0.5
volume 7 scheme sweep source surface 52 target surface 39
mesh volume 7
curve 84 scheme bias 1.05 start vertex 35
curve 79 scheme bias 1.05 start vertex 36
volume 5 size 0.25
volume 5 scheme sweep source surface 36 target surface 23
mesh volume 5
curve 17 scheme bias 1.1 start vertex 11
curve 24 scheme bias 1.1 start vertex 9
curve 34 scheme bias 1.1 start vertex 10
curve 23 scheme bias 1.1 start vertex 12
```

```
curve 18 33 35 22 interval 4
volume 2 size 0.25
volume 2 scheme sweep source surface 7 target surface 11
mesh volume 2
volume 6 size 0.5
volume 6 scheme sweep source surface 39 target surface 47
curve 63 67 interval 4
curve 62 scheme bias 1.1 start vertex 34
curve 60 scheme bias 1.1 start vertex 33
mesh volume 6
volume 4 size 0.25
volume 4 scheme sweep source surface 23
curve 54 58 interval 4
curve 53 scheme bias 1.1 start vertex 35
curve 59 scheme bias 1.1 start vertex 36
mesh volume 4
curve 1 scheme bias 1.1 start vertex 1
curve 5 scheme bias 1.1 start vertex 6
curve 3 scheme bias 1.1 start vertex 4
curve 7 scheme bias 1.1 start vertex 7
curve 10 9 12 11 scheme dualbias 1.1
curve 4 scheme bias 1.1 start vertex 1
curve 6 scheme bias 1.1 start vertex 6
curve 2 scheme bias 1.1 start vertex 2
curve 8 scheme bias 1.1 start vertex 5
volume 1 size 0.3
volume 1 scheme auto
mesh volume 1
curve 174 scheme bias 1.15 start vertex 10
curve 172 scheme bias 1.15 start vertex 36
curve 195 scheme bias 1.05 start vertex 119
curve 197 scheme bias 1.05 start vertex 118
```

```
volume 11 size 0.5
surface 85 scheme pave
volume 11 scheme sweep source surface 85 target surface 87
mesh volume 11
curve 179 scheme bias 1.1 start vertex 119
curve 178 scheme bias 1.1 start vertex 20
volume 10 size 0.3
volume 10 scheme auto
mesh volume 10
block 2 volume 4 5 2 3
block 1 volume 6 7 1 10 11
block 1 2 element type hex8
nodeset 10 surface 5
nodeset 20 surface 2 6 1
nodeset 25 surface 14 81
nodeset 40 surface 85 19 21 9 50 43 37 25 27 45 13 28 46 12
nodeset 50 surface 36 52 22 88
nodeset 30 surface 29 47 11 4 76 89
nodeset 60 surface 77 87
nodeset 100 surface 38 24
sideset 10 surface 5
sideset 20 surface 2 6 1
sideset 25 surface 14 81
sideset 40 surface 85 19 21 9 50 43 37 25 27 45 13 28 46 12
sideset 50 surface 36 52 22 88
sideset 30 surface 29 47 11 4 76 89
sideset 60 surface 77 87
sideset 100 surface 38 24
nodeset 500 curve 174 13 24 33 21
nodeset 600 curve 174
export genesis "edge_coat5.exoII"
```

Aprepro Definitions Include file: (edge_coat5.defs)

```
{scale = 1.0}
{eps = 0.04}
{inlet_plane= (5.0 - eps)/scale}
{die_base = (1.0 -eps)/scale}
{exit_plane = (-7.0/scale)}
{web_plane = 0.0}

{L=.1/scale} cm
{grav = 980} cm/s
{visc = 10.0} P
{density = 1.0 } gm/cm^3
{sig = 50 }  dyne/cm

$ U = {U=1} cm/s
$RE = {Re=density*L*U/visc}
$F = {F=density*grav*L*L/(U*visc)}
$Ca = { U*visc/sig}

$Re = {Re=0.01}
$Ca = {Ca=2.0}
$St = {F=1.01}

$static_angle = {theta_s = 11.4783}
$linear constant = { cT = ( ( cosd(11.4783) - cosd(theta_s))/Ca ) }
```

GOMA input file:

```
{include("edge_coat5.defs")}
```

FEM File Specifications

-- ---- --------------

FEM file	= contin.exoII
Output EXODUS II file	= out.exoII
GUESS file	= contin.dat
SOLN file	= soln.dat
Write intermediate results	= no
Anneal Mesh on Output	= yes

General Specifications

------- --------------

Number of processors	= 1
Output Level	= 0
Debug	= {Debug}
Initial Guess	= read_exoII

Time Integration Specifications

---- ----------- --------------

Time integration	= steady
delta_t	= 5.0e-6
Maximum number of time steps	= 200
Maximum time	= 1
Minimum time step	=1e-9
Maximum time step	=.008
Time step parameter	= 0.5
Time step error	= 1e-1 0 1 1 0 0 0 0
Printing Frequency	= 10
Initial Time	= 0.0

Solver Specifications

------ --------------

Solution Algorithm	= gmres
Preconditioner	= ilut
Matrix Scaling	= row_sum
Matrix reorder	= rcm
Matrix factorization overlap	= none

Matrix ILUT fill factor	= 1.0
Matrix drop tolerance	= 0
Matrix polynomial order	= 3
Size of Krylov subspace	= 600
Orthogonalization	= modified
Maximum Linear Solve Iterations	= 602
Number of Newton Iterations	= 25
Newton correction factor	= 1
Normalized Residual Tolerance	= 1e-7
Residual Ratio Tolerance	= 1e-5
Pressure Stabilization	= yes
Pressure Stabilization Scaling	= 0.10

Boundary Condition Specifications

-------- --------- --------------

Number of BC = -1

#die walls
BC = U NS 20 0.0
BC = V NS 20 0.0
BC = W NS 20 0.0

BC = U NS 25 0.0
BC = V NS 25 0.0
BC = W NS 25 0.0

#inlet
BC = U NS 10 0.0
BC = V NS 10 {-3.50613/1.875/U}
BC = W NS 10 0.0

#symmetry plane
BC = U NS 30 0.0

#free surface
BC = CAPILLARY SS 40 {1.0/Ca} 0. 0. 0.

```
#exit plane

BC = W NS 50 -1.0

#moving web.
BC = U NS 60 0.0
BC = V NS 60 0.0
BC = W NS 60 -1.0

#slip region
BC = V NS 100 0.0
BC = VELO_SLIP SS 100 0.01 0 0 -1

#DCL Edge conditions
BC = VELO_NORMAL_EDGE SS 40 100 0.0
BC = VELO_TANGENT_EDGE SS 40 100 0. 0. -1.0

#MESH conditions

#die walls
BC = DX NS 20 0.0
BC = DY NS 20 0.0
BC = DZ NS 20  0.0

BC = PLANEY SS 25 0. 1. 0. {-die_base}

#Static CL conditions

# Unpinned
BC = CA_EDGE_INT SS 40 25 {theta_s} 0. 1. 0.
BC = DY NS 500 0.0

# To pin static contact line comment out CA_EDGE_INT and
# uncomment the following two.

#BC = DX NS 500  0.0
#BC = DZ NS 500 0.0
```

```
#inlet
BC = PLANEY SS 10 0. 1. 0. {-inlet_plane}

#symmetry plane
BC = PLANEX SS 30 1. 0. 0. 0.

#exit plane
BC = PLANEZ SS 50 0. 0. 1. {-exit_plane}

#moving web
BC = PLANEY SS 60 0. 1. 0. {-web_plane}

#slip region
BC = PLANEY SS 100 0. 1. 0. {-web_plane}

#free surface
BC = KINEMATIC SS 40 0.0

#DCL conditions
BC = VAR_CA_EDGE SS 40 100 {theta_s} {cT} 0. 0. -1.0 0. -1. 0.

#Downstream meniscus is fixed
BC = DY NS 600  0.0
BC = DZ NS 600 0.0

END OF BC


Rotation Specifications =

ROT = MOM EDGE 40 100 VELO_NORMAL_EDGE 40 V 100
VELO_TANGENT_EDGE 40 NONE

ROT = MOM VERTEX 30 40 100 U 30 V 100 VELO_NORMAL_EDGE 40 NONE

ROT = MESH SURFACE 40 T2 0 KINEMATIC 40 T1 0 BASIS_RESEED

ROT = MESH EDGE 40 30 PLANEX 30 KINEMATIC 40 T 0 NONE
```

ROT = MESH EDGE 40 100 VAR_CA_EDGE 40 PLANEY 100 T 0 NONE
ROT = MESH EDGE 40 50 T 0 KINEMATIC 40 PLANEZ 50 NONE
ROT = MESH EDGE 25 40 T 0 DY 500 CA_EDGE_INT 40 NONE

ROT = MESH VERTEX 100 40 30 PLANEX 30 PLANEY 100 VAR_CA_EDGE 40 NONE
ROT = MESH VERTEX 25 40 30 PLANEX 30 PLANEY 25 CA_EDGE_INT 40 NONE
ROT = MESH VERTEX 50 40 100 VAR_CA_EDGE 40 PLANEY 100 PLANEZ 50 NONE
ROT = MESH VERTEX 40 30 50 PLANEX 30 KINEMATIC 40 PLANEZ 50 NONE
ROT = MESH VERTEX 40 30 25 PLANEX 30 DY 600 DZ 600 NONE

END OF ROT

Problem Description
------- -----------
Number of Material = 2
MAT = newt 1
Coordinate System = CARTESIAN
Element Mapping = isoparametric
Mesh Motion = ARBITRARY
Number of bulk species = 0
Number of EQ = 7
EQ = momentum1 Q1 U1 Q1 1 1 1 1 1 0
EQ = momentum2 Q1 U2 Q1 1 1 1 1 1 0
EQ = momentum3 Q1 U3 Q1 1 1 1 1 1 0
EQ = continuity Q1 P Q1 1 0
EQ = mesh1 Q1 D1 Q1 0 0 0 1 0 0
EQ = mesh2 Q1 D2 Q1 0 0 0 1 0 0
EQ = mesh3 Q1 D3 Q1 0 0 0 1 0 0

MAT = stiff_newt 2
Coordinate System = CARTESIAN
Element Mapping = isoparametric
Mesh Motion = ARBITRARY
Number of bulk species = 0
Number of EQ = 7
EQ = momentum1 Q1 U1 Q1 1 1 1 1 1 0
EQ = momentum2 Q1 U2 Q1 1 1 1 1 1 0

```
EQ = momentum3   Q1 U3 Q1   1 1 1 1 1 0
EQ = continuity  Q1 P  Q1   1       0
EQ = mesh1       Q1 D1 Q1   0 0 0 1 0 0
EQ = mesh2       Q1 D2 Q1   0 0 0 1 0 0
EQ = mesh3       Q1 D3 Q1   0 0 0 1 0 0
```

Goma Material file:

```
{include("edge_coat5.defs")}
Material Data File for SAMPLE

/**********Form of each property card *********/
PROPERTY    = MODEL    FLOAT#1 FLOAT#2 .....FLOAT#5
/**********Form of each Constitutive card *********/
MECHANICS_TYPE      = MODEL
Of the many available options, MODEL can be USER
/***********************************************/

---Physical Properties
Density              = CONSTANT      {Re}

---Mechanical Properties and Constitutive Equations
Solid Constitutive Equation     = NONLINEAR
Convective Lagrangian Velocity = NONE

Lame MU                    = CONSTANT      0.1
Lame LAMBDA                = CONSTANT      1.0
#
# the following two cards are used to create the stiffer
# pseudo-solid material adjacent to the contact lines.
#
#Lame MU                   = CONSTANT      10000.0
#Lame LAMBDA               = CONSTANT      1.0
Stress Free Solvent Vol Frac    = CONSTANT      0.0
Liquid Constitutive Equation    = NEWTONIAN
Viscosity                  = CONSTANT      1.0
Polymer Constitutive Equation   = NOPOLYMER
```

#Surface Tension = CONSTANT {1./Ca}

---Thermal Properties
Conductivity = CONSTANT 1.
Heat Capacity = CONSTANT 1.
Volume Expansion = CONSTANT 1.
Reference Temperature = CONSTANT 0.
Liquidus Temperature = CONSTANT 1.
Solidus Temperature = CONSTANT 1.

---Electrical Properties
#Electrical Conductivity = CONSTANT 100.
Electrical Conductivity = CONSTANT .0943

---Microstructure Properties
Media Type = CONTINUOUS
Porosity = CONSTANT 0.9
Permeability = CONSTANT 1.0
FlowingLiquid Viscosity = CONSTANT 1.0
Inertia Coefficient = CONSTANT 0.0

---Species Properties
Diffusion Constitutive Equation = FICKIAN
Diffusivity = CONSTANT 0 0.10
#Species Time Integration = TAYLOR_GALERKIN_EXP 0
#Species Time Integration = TAYLOR_GALERKIN 0
Species Time Integration = STANDARD 0
Latent Heat Vaporization = CONSTANT 0 0.
Latent Heat Fusion = CONSTANT 0 0.
Vapor Pressure = CONSTANT 0 0.
Species Volume Expansion = CONSTANT 0 0.
Reference Concentration = CONSTANT 0 0.

********Species Number**********|

----Source Terms
Navier-Stokes Source = CONSTANT 0.0 {-F} 0.0

Solid Body Source = CONSTANT 0. 0. 0.
Mass Source = CONSTANT 0.
Heat Source = CONSTANT 0.
Species Source = CONSTANT 0 0.
Current Source = CONSTANT 0.

TAB:9114:tab